Supporting Information

In-Situ 2D-Perovskite-Like Ligand Offers Versatile Passivation of Large and Small Sized PbS Quantum Dots for Infrared Photovoltaics

Kai Liao,[1⊥] Beining Dong,[2⊥] Yajie Yan,[1] Xiaoxiao Zhang,[1] Kou Li[2], Dewei Chu[2], Long Hu,[2,*] and Ziqi Liang[1,*]

[*][1]Prof. Z. Liang, K. Liao, Dr. Y. Yan, X. Zhang
Department of Materials Science
Fudan University
Shanghai 200433, China
Email: zqliang@fudan.edu.cn

[*][2]Dr. L. Hu, B. Dong, K. Li, Prof. D. Chu
School of Materials Science and Engineering
University of New South Wales (UNSW)
Sydney, NSW 2052, Australia
Email: long.hu@unsw.edu.au

[⊥]K. Liao and B. Dong equally contributed to this work.

Keywords: PbS quantum dots, 2D perovskite precursor, solution-phase ligand-exchange, colloidal stability, solar cells

Experimental Section

Materials: PbI_2 (99.9%) and *n*-BAI (99.5%) were purchased from Maituowei Ltd. (China). PbO (99.97%), OA (99%), ODE (>90%), $(TMS)_2S$ (>97%), 1,2-ethylenedithiol (EDT, 97%), *n*-BA (≥99.7%) and *N*,*N*-dimethylformamide (DMF, 99.8%) were purchased from Aladdin. Acetonitrile (≥99.0%), *n*-hexane (99.7%), methanol (99.7%), Ammonium acetate (97%) and ethanol (99.7%) were purchased from Sinopharm. Toluene (99.7%) were purchased from Dahe, Ltd. (China).

Synthesis of PbS CQDs: OA-capped PbS CQDs with an exciton peak of 1180 nm were synthesized according to previous reports.[S1] Lead oxide (0.45 g), oleic acid (3 mL), and octadecene (20 mL) were mixed in a three-neck flask and heated to 150 ℃ in Ar atmosphere for 2 h. Then, 0.24 mL Bis(trimethylsilyl)sulfide dissolved in 8 mL of octadecene was then injected rapidly into the flask. The CQD solution was slowly cooled to room temperature followed by injecting 20 mL of *n*-hexane. Ethanol was added to precipitate the CQD solution, which was then redispersed in *n*-hexane. The CQDs were further purified twice by adding ethanol. Finally, the CQDs were dissolved in *n*-hexane solution with a

concentration of 50 mg mL^{-1}. OA-capped PbS CQDs with an exciton peak of 933nm were synthesized under the identical conditions except the injection temperature of 90 °C.

Ligand Exchange of PbS CQDs Solution: The both types of 1.0 eV-CQD and 1.3 eV-CQD octane solutions were diluted to ≈10 mg ml^{-1} and filtered using a filter with a pore size of 0.2 μm. 10 mL of diluted CQD solution was added to 10 mL of DMF solvent containing 0.1 M PbI_2 and 0.2 M BAI and 0.04 M ammonium acetate. The mixed solution was stirred vigorously for 3 min at room temperature for ligand exchange. After 5 min, the CQDs were transferred to DMF solution from octane solution. The octane solution was decanted and the CQD in DMF was washed twice with octane to adequately remove residual oleic acid ligands. CQDs were precipitated by adding 10 mL toluene and collected by centrifugation. The solids were then dried for 15 min in the vacuum oven and stored in Ar-filled glovebox.

Solution and Thin-Film Characterization: The dried CQD solids were redispersed in BA (250 mg mL^{-1}) for film by spin coating at 2500 rpm for 30 s, followed by thermal annealing at 70 °C for 10 min in Ar-filled glove box to remove solvent residues and yield PbS CQDs thin films. Optical absorption spectra of samples were acquired on Hitachi U-4100 UV-Visible spectrophotometer. Steady-state photoluminescence was measured using Edinburgh FLS1000 Fluorescence Spectrometers with the excitation beam at 430 nm. The PL intensity was then corrected by absorbed photon numbers at the exciting light wavelength. Transmission electron microscopic (TEM) imaging was performed on JEM-2100F (JEOL Ltd.) at an accelerating voltage of 200 kV. FT-IR spectra were acquired by beamline BL01B at Shanghai Synchrotron Radiation Facility (SSRF), and the powder samples were obtained by redrying the as-prepared solutions. The FTIR spectrum in Figure 3a was obtained from vacuum-dried PbS-OA and PbS-$(BA)_2PbI_4$ samples, demonstrating whether $(BA)_2PbI_4$ was successfully exchanged. The FTIR spectrum in Figure S4 characterizes the compositional changes of PbS-$(BA)_2PbI_4$ before and after annealing to investigate its crystallization behavior. 1HNMR spectra were acquired by AVANCE III HD 400 (Nasdaq:BRKR) in dimethyl sulfoxide-d6 solution at room temperature. X-ray diffraction pattern data for 2θ values were collected with a Rigaku SmartLab9KW diffractometer with nickel filtered Cu Kα radiation (λ = 1.5406 Å). GIWAXS patterns were acquired by beamline BL14B1 at SSRF with an X-ray source of 10 keV and incident angle of 0.2°, and the measured spectra were further corrected by a MATLAB toolbox of GIXSGUI. X-ray photoelectron spectroscopy (XPS) spectra were acquired on a ESCALAB 250 spectrometer with a source gun type of Al Kα and an energy step of 0.05 eV. The laser pulse width was 130 fs and the repetition rate was 100 m Hz. The excitation wavelength for TRPL measurements is 600 nm. Ultraviolet photoemission spectroscopy (UPS) measurements were carried out in a Kratos AXIS Ultra-DLD ultrahigh vacuum photoemission spectroscopy system with an Al Kα radiation source

Device Fabrication and Measurements: ITO substrates (15 Ω/square) were cleaned sequentially with water, acetone, and isopropyl alcohol with an ultrasonic bath for 20 min and dried with air flow. The substrates were treated with UV-ozone for 20 min before ZnO layer deposition. The ZnO precursor solution was prepared by dissolving 200 mg zinc acetate dihydrate into 2 mL of 2-methoxyethanol and 60 μL of 2-aminoethanol and stirred at room temperature overnight. In air, ZnO precursor solution was spin-coated at 5000 rpm and annealed at 200 °C for 30 min. Then samples were transferred into glovebox. The CQD solid films were obtained following the film fabrication process above. Then the hole-transport layer (HTL) (~50 nm in thickness) was two layers of PbS CQD ligand exchanged by 1,2-ethanedithiol (EDT) (0.02 vol% in acetonitrile). In each layer, CQDs capped with oleic acid (20 mg ml^{-1}) were spun cast, followed by a 30 s soaking in diluted EDT (0.02 vol% in acetonitrile) and three washings with acetonitrile. Finally, samples were transferred into a thermal evaporator to deposit 100 nm Au layers with electrode shadow mask under a vacuum of 10^{-5} Torr. The active area as defined shadow mask is ~0.04 cm^2. The sample was mounted inside an argon-filled sample holder with a quartz optical window for subsequent measurements. The device reproducibility is improved by strictly maintaining the moisture/oxygen ratio and temperature in the inert atmosphere glovebox. The light *J–V* curves were measured on a Keithley 2400 source meter unit under AM 1.5G light illumination with a Newport-Oriel (Sol3A Class AAA Solar Simulator, 94043A) solar simulator operating at an intensity of 100 mW cm^{-2}. The light intensity was calibrated by a certified Oriel reference cell (91150V) and verified with a NREL calibrated, filtered Si diode (Hamamatsu, S1787-04). The J–V profiles were obtained under both forward (−0.2 V → +0.8 V) and reverse (+0.8 V → −0.2 V) scans. Device annealing for stability test was conducted in air with relatively humidity of 65%.

DFT Simulation: DFT calculations were performed by using the Vienna Ab-initio Simulation Package (VASP).[S2,S3] The exchange–correlation interactions were described by generalized gradient approximation (GGA) with the Perdew–Burke–Ernzerhof (PBE) functional.[S4,S5] Spin-polarization was included in all the calculations and a damped van der Waals correction was incorporated using Grimme's scheme to better describe the non-bonding interactions.[S6] The cut-off energies for plane waves were set to be 500 eV, and the residual force and energy on each atom during structure relaxation were converged to 0.005 eV $Å^{-1}$ and 10^{-5} eV, respectively.

The adsorption energy (E_{ad}) is defined as $E_{ad} = E_{PbS(100)+ads} - E_{ads} - E_{PbS(100)}$ where $E_{PbS(100)+ads}$ is the total energy of PbS(100) adsorbed with $BA^+/MA^+/I^-$, E_{ads} is the total energy of $BA^+/MA^+/I^-$, $E_{PbS(100)}$ is the total energy of PbS(100).

Supplementary Figures

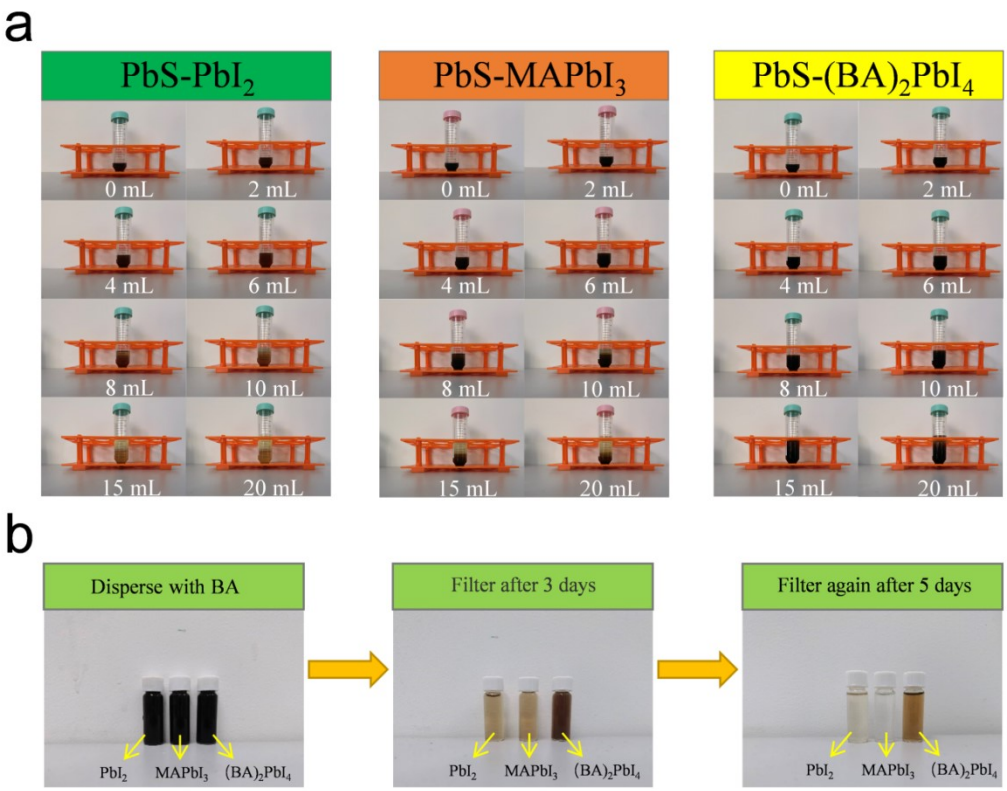

Figure S1. Comparison of solution stability of CQDs capped by PbI_2, $MAPbI_3$ and $(BA)_2PbI_4$ via (a) ligand-exchanging followed by purification with different volumes of toluene as anti-solvent, and (b) dispersion in BA solvent with filtration after 3 and 5 days, respectively.

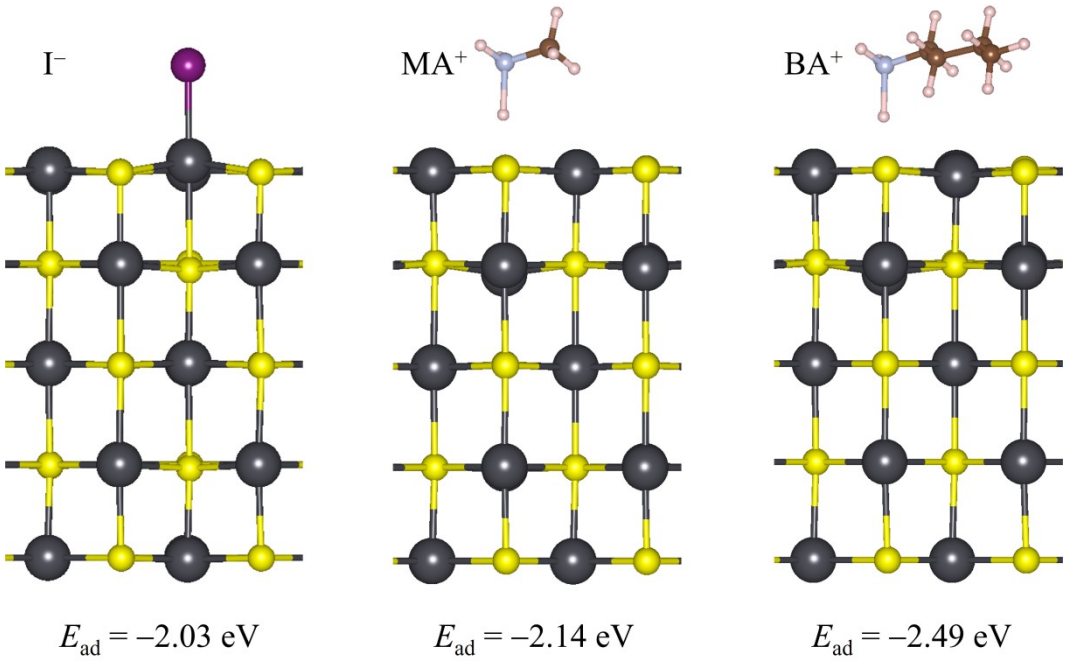

Figure S2. Chemical structures of I^-, MA^+, BA^+ ligands and their adsorption energy to PbS (100) facets.

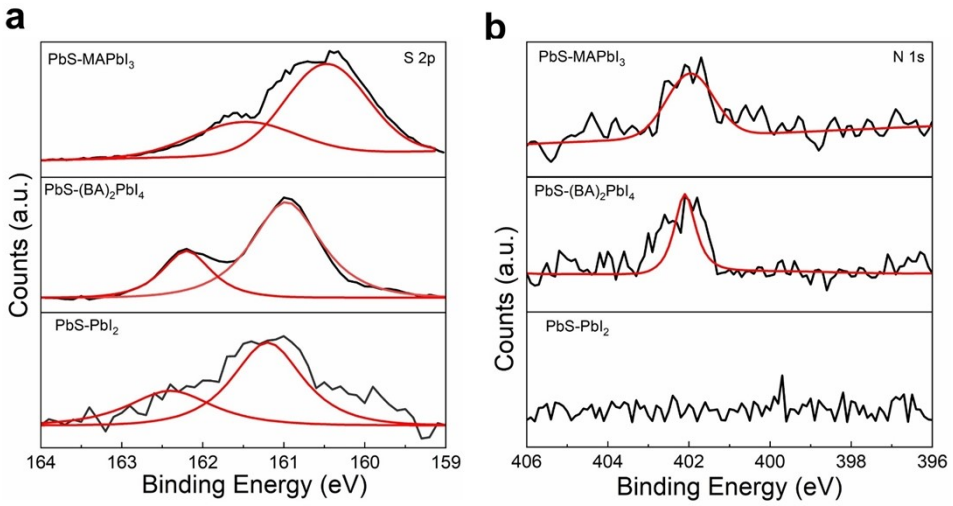

Figure S3. XPS profiles of PbS-$MAPbI_3$, PbS-$(BA)_2PbI_4$, PbS-PbI_2 samples, showing (a) S 2*p* and (b) N 1*s* core.spectra.

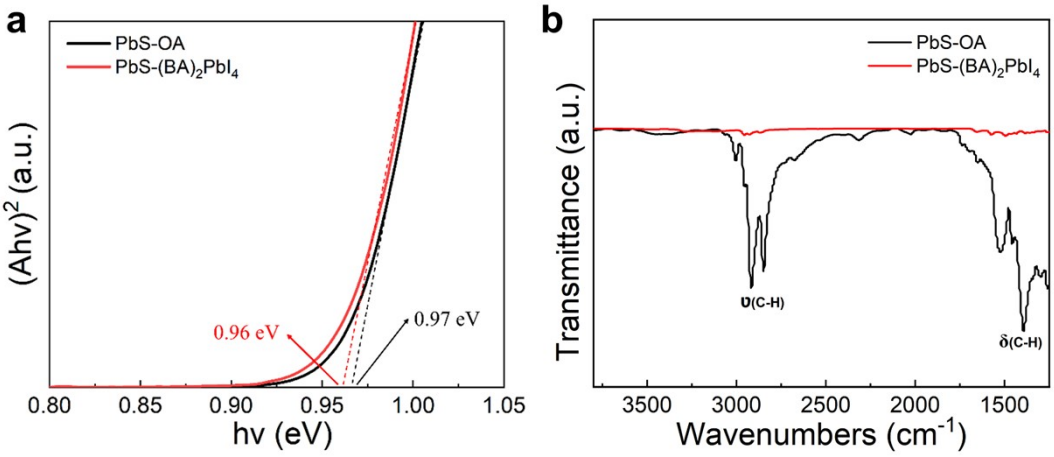

Figure S4. (a) Bandgap calculation of PbS-OA and PbS-$(BA)_2PbI_4$ CQDs via Tauc Plot method. (b) FTIR spectra of PbS CQDs before and after ligand-exchange.

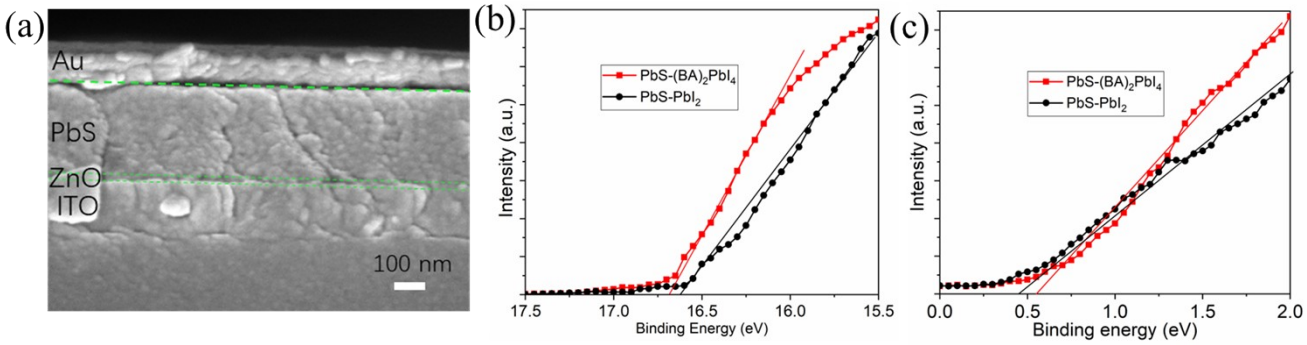

Figure S5. (a) Cross-sectional SEM image of a whole device of PbS-$(BA)_2PBI_4$. (b) Magnified UPS spectra showing secondary edge (E_{SE}) for determining the work function (WF) and Fermi level (E_F) using Equation 1. (c) The magnified UPS spectra showing the onset energy (E_{onset}) to determine valence band maximum energy.

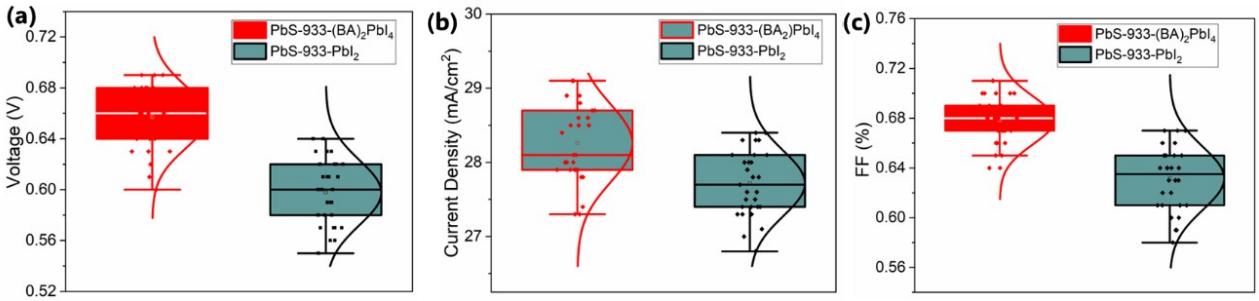

Figure S6. The statistics of V_{OC}, J_{SC} and FF for both types of solar cell of PbS-933-$(BA)_2PbI_4$ and PbS-933-PbI_2.

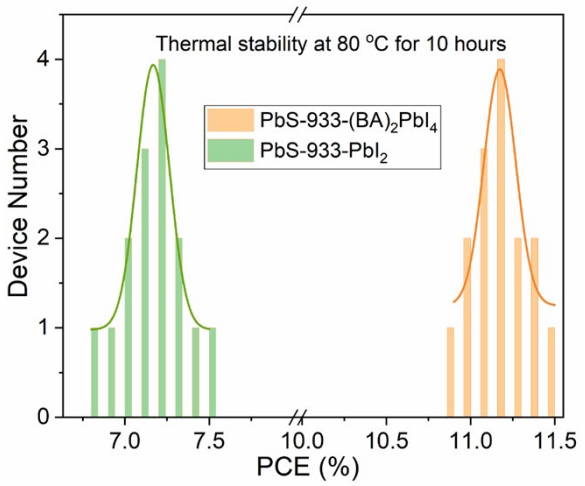

Figure S7. PCE distribution of solar cells based on 933 nm-PbS CQDs for thermal stability comparison after 10-hour heating at 80 °C in air.

Supplementary References

[S1] Y. Liu, H. Wu, G. Shi, Y. Li, Y. Gao, S. Fang, H. Tang, W. Chen, T. Ma, I. Khan, K. Wang, C. Wang, X. Li, Q. Shen, Z. Liu, W. Ma, Merging Passivation in Synthesis Enabling the Lowest Open-Circuit Voltage Loss for PbS Quantum Dot Solar Cells. *Adv. Mater.* **2022**, *35*, 2207293.

[S2] G. Kresse, J. Furthmüller, Efficiency of Ab-Initio Total Energy Calculations for Metals and Semiconductors Using a Plane-Wave Basis Set. *Comput. Mater. Sci.* **1996**, *6*, 15–50.

[S3] G. Kresse and J. Furthmüller, Efficient Iterative Schemes for Ab Initio Total-Energy Calculations Using a Plane-Wave Basis Set. *Phys. Rev. B.* **1996**, *54*, 11169–11186.

[S4] J. P. Perdew, K. Burke, M. Ernzerhof, Generalized Gradient Approximation Made Simple. *Phys. Rev. Lett.* **1996**, *77*, 3865–3868.

[S5] J. P. Perdew, M. Ernzerhof, K. Burke, Rationale for Mixing Exact Exchange with Density Functional Approximations. *J. Chem. Phys.* **1996**, *105*, 9982–9985.

[S6] S. Grimme, Semiempirical GGA-type Density Functional Constructed with a Long-Range Dispersion Correction. *J. Comput. Chem.* **2006**, *27*, 1787–1799.